

## The Jacobi polynomials QCD analysis for the polarized structure function

---

S. Atashbar Tehrani<sup>ac</sup> and Ali N. Khorramian<sup>bc</sup>

<sup>a</sup>*Physics Department, Persian Gulf University,  
P.O.Box 75169-13798, Boushehr, Iran*

<sup>b</sup>*Physics Department, Semnan University,  
P.O.Box 35195-363, Semnan, Iran*

<sup>c</sup>*Institute for Studies in Theoretical Physics and Mathematics (IPM),  
P.O.Box 19395-5531, Tehran, Iran*

*E-mail: atashbar@ipm.ir, khorramiana@theory.ipm.ac.ir*

ABSTRACT: We present the results of our QCD analysis for polarized quark distribution and structure function  $xg_1(x, Q^2)$ . We use very recently experimental data to parameterize our model. New parameterizations are derived for the quark and gluon distributions for the kinematic range  $x \in [10^{-8}, 1]$ ,  $Q^2 \in [1, 10^6] \text{ GeV}^2$ . The analysis is based on the Jacobi polynomials expansion of the polarized structure functions. Our calculations for polarized parton distribution functions based on the Jacobi polynomials method are in good agreement with the other theoretical models. The values of  $\Lambda_{\text{QCD}}$  and  $\alpha_s(M_z)$  are determined.

KEYWORDS: Phenomenological Models, NLO Computations, Spin and Polarization Effects, Deep Inelastic Scattering.

---

## Contents

|   |          |
|---|----------|
| <b>1. Introduction</b>  | <b>1</b> |
| <b>2. Polarized valon distributions</b>                           | <b>2</b> |
| <b>3. The theoretical background of the QCD analysis</b>          | <b>5</b> |
| <b>4. The method of the QCD analysis of PSF</b>                   | <b>7</b> |
| <b>5. The procedure of the QCD fit of <math>g_1^p</math> data</b> | <b>8</b> |
| <b>6. Results and conclusions of the QCD analysis</b>             | <b>9</b> |

---

## 1. Introduction

The nature of the short-distance structure of polarized nucleons is one of the central questions of present day hadron physics. For more than sixteen years, polarized inclusive deep inelastic scattering has been the main source of information on how the individual partons in the nucleon are polarized at very short distances.

The theoretical and experimental status on the spin structure of the nucleon has been discussed in great detail in several recent reviews (see, e.g., refs. [1–4]). During the recent years several comprehensive analysis of the polarized deep inelastic scattering (DIS) data, based on next-to-leading-order quantum chromodynamics, have appeared in refs.[5-29]. In these analysis the polarized parton density functions (PPDFs) are either written in terms of the well-known parameterizations of the unpolarized PDFs or parameterized independently, and the unknown parameters are determined by fitting the polarized DIS data.

Determination of parton distributions in a nucleon in the framework of quantum chromodynamics (QCD) always involves some model-dependent procedure. Instead of relying on mathematical simplicity as a guide, we take a viewpoint in which the physical picture of the nucleon structure is emphasized. That is, we consider the model for the nucleon which is compatible with the description of the bound state problem in terms of three constituent quarks. We adopt the view that these constituent quarks in the scattering problems should be regarded as the valence quark clusters rather than point-like objects. They have been referred to as *valons*. In the valon model, the proton consists of two “up” and one “down” valons. These valons thus, carry the quantum numbers of the respective valence quarks. Hwa and et al. [30-38] found evidence for the valons in the deep inelastic neutrino scattering data, suggested their existence and applied it to a variety of phenomena. Hwa [39] has also successfully formulated a treatment of the low- $p_T$  reactions based

on a structural analysis of the valons. In [40] Hwa and Yang refined the idea of the valon model and extracted new results for the valon distributions. In [41–43] unpolarized PDFs and hadronic structure functions in the NLO approximation were extracted.

In ref. [25] the polarized valon model is applied to determine the quark helicity distributions and polarized proton structure functions in the NLO approximation by using the Bernstein polynomial approach.

The extraction of the quark helicity distributions is one of the main tasks of the semi-inclusive deep inelastic scattering (SIDIS) experiments (HERMES [44], COMPASS [45], SMC [46]) with the polarized beam and target. Recently in ref. [28] the polarized valon model was applied and analyzed the flavor-broken light sea quark helicity distributions with the help of a Pauli-blocking ansatz. The results reported of this paper is good agreement with the HERMES experimental data for the quark helicity distributions in the nucleon for up, down, and strange quarks from semi-inclusive deep-inelastic scattering [44]. The reported results of ref. [44] is based on the Bernstein polynomial expansion method in the polarized valon model framework.

Since very recently experimental data are available from the HERMES collaboration [47] for the spin structure function  $g_1$ , therefore there is enough motivation to study and utilize the spin structure and quark helicity distributions extracted via the phenomenological model. Since these recently experimental data are just for different value of  $Q^2$  and not fixed  $Q^2$ , one can not use the the Bernstein polynomial expansion method. Because in this method we need to use experimental data for each bin of  $Q^2$  separately. So it seems suitable, to use the Jacobi polynomial expansion method.

In this paper we use the idea of the polarized valon model to obtain the PPDFs in the LO and NLO approximations. The results of the present analysis is based on the Jacobi polynomials expansion of the polarized structure function.

The plan of the paper is to give an introduction to the polarized valon distributions in section 2. Parametrization of parton densities are written down in this section. In section 3 we present a brief review of the theoretical background of the QCD analysis in two loops. The method of the QCD analysis of polarized structure function, based on Jacobi polynomials are written down in section 4. A description of the procedure of the QCD fit of  $g_1$  data are illustrated in section 5. section 6 contains a results and conclusions of the QCD analysis.

## 2. Polarized valon distributions

The idea of nucleon as a bound state of three quarks was presented for the first time in ref. [48]. On the other hand the similar idea, which is called valon model was presented in ref. [37]. According to the valon model framework, one can assume a simple form for the exclusive valon distribution which facilitate the phenomenological analysis as follows

$$G_{UUD/p}(y_1, y_2, y_3) = g(y_1 y_2)^a y_3^b \delta(y_1 + y_2 + y_3 - 1) , \quad (2.1)$$

where  $y_i$  is the momentum fraction of the  $i$ 'th valon. The  $U$  and  $D$  type inclusive valon distributions can be obtained by double integration over the unspecified variables

$$G_{U/p}(y) = \int dy_2 \int dy_3 G_{UUD/p}(y, y_2, y_3) = gB(a+1, b+1)y^a(1-y)^{a+b+1}, \quad (2.2)$$

$$G_{D/p}(y) = \int dy_1 \int dy_2 G_{UUD/p}(y_1, y_2, y) = gB(a+1, a+1)y^b(1-y)^{2a+1}. \quad (2.3)$$

The normalization parameter  $g$  has been fixed by

$$\int_0^1 G_{U/p}(y)dy = \int_0^1 G_{D/p}(y)dy = 1, \quad (2.4)$$

and is equal to  $g = [B(a+1, b+1)B(a+1, a+b+2)]^{-1}$ , where  $B(m, n)$  is the Euler-Beta function. R.C. Hwa and C. B. Yang [40] have recalculated the unpolarized valon distribution in the proton with a new set of parameters. The new values of  $a$ ,  $b$  are found to be  $a = 1.76$  and  $b = 1.05$ .

To describe the quark distribution  $q(x)$  in the valon model, one can try to relate the polarized quark distribution functions  $q^\uparrow$  or  $q^\downarrow$  to the corresponding valon distributions  $G^\uparrow$  and  $G^\downarrow$ . The polarized valon can still have the valence and sea quarks that are polarized in various directions, so long as the net polarization is that of the valon. When we have only one distribution  $q(x, Q^2)$  to analyze, it is sensible to use the convolution in the valon model to describe the proton structure in terms of the valons. In the case that we have two quantities, unpolarized and polarized distributions, there is a choice of which linear combination exhibits more physical contents. Therefore, in our calculations we assume a linear combination of  $G^\uparrow$  and  $G^\downarrow$  to determine respectively the unpolarized ( $G$ ) and polarized ( $\Delta G$ ) valon distributions.

According to unpolarized and polarized valon model framework we have [25]

$$q_{i/p}(x, Q^2) = \sum_j \int_x^1 q_{i/j}\left(\frac{x}{y}, Q^2\right) G_{j/p}(y) \frac{dy}{y}, \quad (2.5)$$

and

$$\Delta q_{i/p}(x, Q^2) = \sum_j \int_x^1 \Delta q_{i/j}\left(\frac{x}{y}, Q^2\right) \Delta G_{j/p}(y) \frac{dy}{y}. \quad (2.6)$$

where  $q_i \equiv q_i^\uparrow + q_i^\downarrow$  and  $\Delta q_i \equiv q_i^\uparrow - q_i^\downarrow$  and also  $G_j \equiv G_j^\uparrow + G_j^\downarrow$  and  $\Delta G_j \equiv G_j^\uparrow - G_j^\downarrow$ . As we can similarly see for the unpolarized case, the polarized quark distribution can be related to a polarized valon distribution in eq. (2.6).

The polarized parton distribution of the polarized constituent quarks in the eq. (2.6) is dependent on a probe [25]. It is assumed in more detail that the polarized constituent quarks distribution, that is,  $\Delta q_{i/j}(z = \frac{x}{y}, Q^2)$  in the scale of  $Q_0^2$  is equal to  $\Delta q_{i/j}(z, Q_0^2) = \delta(1-z)$ . From eq. (2.6) now is obvious that the polarized quark distribution in the scale of  $Q_0^2$  is equal to polarized valon distribution.

Here we want to use the polarized valon distributions which introduced in [25]. According to improve polarized valon picture the nonsinglet polarized valon distribution functions are as following

$$\Delta G_j(y) = \Delta \mathcal{W}_j(y) \times G_j(y), \quad (2.7)$$

where

$$\Delta \mathcal{W}_j(y) = \xi_j A_j y^{\alpha_j} (1-y)^{\beta_j} (1 + \gamma_j y + \eta_j y^{0.5}), \quad (2.8)$$

the subscript  $j$  refers to  $U$  and  $D$ -valons. The motivation for choosing this functional form is that the  $y^{\alpha_j}$  term controls the low- $y$  behavior valon densities, and  $(1-y)^{\beta_j}$  terms the large- $y$  values. The remaining polynomial factor accounts for the additional medium- $y$  values. The normalization constants  $A_j$  for  $U$  and  $D$ -valons are as following

$$A_U^{-1} = [B(a + \alpha_U, 2 + a + b + \beta_U) + \eta_U B(0.5 + a + \alpha_U, 2 + a + b + \beta_U) + \gamma_U B(1 + a + \alpha_U, 2 + a + b + \beta_U)] / B(1 + a, 2 + a + b), \quad (2.9)$$

and

$$A_D^{-1} = [B(b + \alpha_D, 2 + 2a + \beta_D) + \eta_D B(0.5 + b + \alpha_D, 2 + 2a + \beta_D) + \gamma_D B(1 + b + \alpha_D, 2 + 2a + \beta_D)] / B(b + 1, 2a + 2). \quad (2.10)$$

These quantities are chosen such that the  $\xi_j$  are the first moments of  $\Delta G_j(y)$ ,  $\xi_j = \int_0^1 dy \Delta G_j(y)$ . Here  $B(a, b)$  is the Euler Beta-function being related to the  $\Gamma$ -function.

In the present approach the QCD-evolution equations are solved in MELLIN- $N$  space as will describe in section 3. The MELLIN-transform of the valon densities is performed and MELLIN- $N$  moments are calculated for complex arguments  $N$  by  $\int_0^1 y^{N-1} \Delta G_{j/p}(y) dy$ .

As seen from eq. (2.7) there are five parameters for each valon distribution. To meet both the quality of the present data and the reliability of the fitting program, the number of parameters has to be reduced. Assuming SU(3) flavor symmetry and a flavor symmetric sea one only has to derive one general polarized sea-quark distribution. The first moments of the polarized valon distributions  $\Delta G_U$  and  $\Delta G_D$  can be fixed by the SU(3) parameters  $F$  and  $D$  as measured in neutron and hyperon  $\beta$ -decays according to the relations :

$$\begin{aligned} 2\xi_U - \xi_D &= F + D, \\ 2\xi_U + \xi_D &= 3F - D. \end{aligned} \quad (2.11)$$

The factor 2 in eq. (2.11) is due to the existence of two- $U$  type valons. A re-evaluation of  $F$  and  $D$  was performed in ref. [24] on the basis of updated  $\beta$ -decay constants [49] leading to

$$\begin{aligned} 2\xi_U &= 0.926 \pm 0.014, \\ \xi_D &= -0.341 \pm 0.018. \end{aligned} \quad (2.12)$$

This choice reduces the number of parameters to be fitted for each nonsinglet valon density to four.

On the other hand the singlet polarized valon distribution which is defined in [25] is as following

$$\Delta G'_j(y) = \Delta \mathcal{W}'_j(y) \times G_j(y) \tag{2.13}$$

where  $\Delta \mathcal{W}'_j(y)$  in eq. (2.13) has the following form

$$\Delta \mathcal{W}'_j(y) = \Delta \mathcal{W}_j(y) \times \sum_{m=0}^5 \mathcal{A}_m y^{\frac{m-1}{2}}. \tag{2.14}$$

The additional term in the above equation, ( $\sum$  term), serves to control the behavior of the singlet sector at very low- $y$  values and the  $\Delta \mathcal{W}_j(y)$  defined in eq. (2.8).

In the next sections we need to use the MELLIN moments of eqs. (2.7), (2.13) to determine MELLIN moments of PDFs in our analysis.

### 3. The theoretical background of the QCD analysis

Let us define the MELLIN moments for the polarized structure function  $g_1^p(x, Q^2)$ :

$$g_1^p(N, Q^2) = \int_0^1 x^{N-1} g_1^p(x, Q^2) dx \tag{3.1}$$

In the QCD-improved quark parton model (QPM), i.e., at leading twist, and to leading logarithmic order in the running strong coupling constant  $\alpha_s(Q^2)$  of Quantum-Chromodynamics (LO QCD), the deep-inelastic scattering off the nucleon can be interpreted as the incoherent superposition of virtual-photon interactions with quarks of any flavor  $q$ . By angular momentum conservation, a spin- $\frac{1}{2}$  parton can absorb a hard photon only when their spin orientations are opposite. The spin structure function  $g_1$  has then a probabilistic interpretation, which for the proton reads [50]

$$\begin{aligned} g_1^p(N, Q^2) &= \frac{1}{2} \sum_q e_q^2 [\Delta q(N, Q^2) + \Delta \bar{q}(N, Q^2)] \\ &= \frac{1}{2} \langle e^2 \rangle [\Delta q_S(N, Q^2) + \Delta q_{NS}(N, Q^2)]. \end{aligned} \tag{3.2}$$

Here, the quantity  $-Q^2$  is the squared four-momentum transferred by the virtual photon,  $N$  is the order of moments,  $e_q$  is the charge, in units of the elementary charge  $|e|$ , of quarks of flavor  $q$ ,  $\langle e^2 \rangle = \sum_q e_q^2 / N_q$  is the average squared charge of the  $N_q$  active quark flavors, and  $\Delta q(N, Q^2)$  is the quark helicity distribution for quarks of flavor  $q$ . Correspondingly,  $\Delta \bar{q}(N, Q^2)$  is anti-quark helicity distributions. Moreover the flavor singlet and flavor non-singlet quark helicity distributions are defined as

$$\begin{aligned} \Delta q_S(N, Q^2) &= \sum_q [\Delta q(N, Q^2) + \Delta \bar{q}(N, Q^2)] \\ &\equiv \Delta \Sigma(N, Q^2), \end{aligned} \tag{3.3}$$

and

$$\Delta q_{NS}(N, Q^2) = \frac{1}{\langle e^2 \rangle} \sum_q e_q^2 [\Delta q(N, Q^2) + \Delta \bar{q}(N, Q^2)] - \Delta q_S(N, Q^2). \tag{3.4}$$

For the analysis presented in this paper, only the three lightest quark flavors,  $q = u, d, s$ , are taken into account and the number of active quark flavors  $N_q$  is equal to three.

The twist-2 contributions to the structure function  $g_1(N, Q^2)$  can be represented in terms of the polarized parton densities and the coefficient functions  $\Delta C_i^N$  in the MELLIN-N space by [2]

$$g_1^p(N, Q^2) = \frac{1}{2} \sum_q e_q^2 \left\{ \left( 1 + \frac{\alpha_s}{2\pi} \Delta C_q^N \right) [\Delta q(N, Q^2) + \Delta \bar{q}(N, Q^2)] + \frac{\alpha_s}{2\pi} 2\Delta C_g^N \Delta g(N, Q^2) \right\}, \quad (3.5)$$

in this equation the NLO running coupling constant is given by

$$\alpha_s(Q^2) \cong \frac{1}{b \log \frac{Q^2}{\Lambda_{\overline{MS}}^2}} - \frac{b' \ln \left( \ln \frac{Q^2}{\Lambda_{\overline{MS}}^2} \right)}{b^3 \left( \ln \frac{Q^2}{\Lambda_{\overline{MS}}^2} \right)^2}, \quad (3.6)$$

where  $b = \frac{33-2f}{12\pi}$  and  $b' = \frac{153-19f}{24\pi^2}$ . In the above equations, we choose  $Q_0 = 1 \text{ GeV}^2$  as a fixed parameter and  $\Lambda$  is an unknown parameter which can be obtained by fitting to experimental data.

In eq. (3.5),  $\Delta q(N, Q^2) = \Delta q_v(N, Q^2) + \Delta \bar{q}(N, Q^2)$ ,  $\Delta \bar{q}(N, Q^2)$  and  $\Delta g(N, Q^2)$  are moments of the polarized parton distributions in a proton.  $\Delta C_q^N$ ,  $\Delta C_g^N$  are also the  $N$ -th moments of spin-dependent Wilson coefficients given by

$$\Delta C_q^N = \frac{4}{3} \left[ -S_2(N) + (S_1(N))^2 + \left( \frac{3}{2} - \frac{1}{N(N+1)} \right) S_1(N) + \frac{1}{N^2} + \frac{1}{2N} + \frac{1}{N+1} - \frac{9}{2} \right], \quad (3.7)$$

and

$$\Delta C_g^N = \frac{1}{2} \left[ -\frac{N-1}{N(N+1)} (S_1(N) + 1) - \frac{1}{N^2} + \frac{2}{N(N+1)} \right], \quad (3.8)$$

with  $S_k(N)$  defined as in ref. [2].

According to improved polarized valon model framework, determination of the moments of parton distributions in a proton can be done strictly through the moments of the polarized valon distributions.

The moments of PPDFs are denoted respectively by:  $\Delta u_v(N, Q^2)$ ,  $\Delta d_v(N, Q^2)$ ,  $\Delta \Sigma(N, Q^2)$  and  $\Delta g(N, Q^2)$ . Therefore, the moments of the polarized  $u$  and  $d$ -valence quark in a proton are convolutions of two moments:

$$\Delta u_v(N, Q^2) = 2\Delta M^{\text{NS}}(N, Q^2) \times \Delta M'_{U/p}(N), \quad (3.9)$$

$$\Delta d_v(N, Q^2) = \Delta M^{\text{NS}}(N, Q^2) \times \Delta M'_{D/p}(N), \quad (3.10)$$

In the above equation  $M'_{j/p}(N)$  is the moment of  $\Delta G_{j/p}(y)$  distribution, i.e.  $\Delta M'_{j/p}(N) = \int_0^1 y^{N-1} \Delta G_{j/p}(y) dy$ .

The moment of the polarized singlet distribution ( $\Sigma$ ) is as follows:

$$\Delta \Sigma(N, Q^2) = \Delta M^S(N, Q^2) (2\Delta M''_{U/p}(N) + \Delta M''_{D/p}(N)). \quad (3.11)$$

here  $M''_{j/p}(N)$  is the moment of  $\Delta G'_{j/p}(y)$  distribution, i.e.  $\Delta M''_{j/p}(N) = \int_0^1 y^{N-1} \Delta \cdot G'_{j/p}(y) dy$ . For the gluon distribution we have

$$\Delta g(N, Q^2) = \Delta M^{gq}(N, Q^2)(2\Delta M'_{U/p}(N) + \Delta M'_{D/p}(N)), \quad (3.12)$$

where  $\Delta M^{\text{NS}}(N, Q^2)$  in eqs. (3.9), (3.10),  $\Delta M^S(N, Q^2)$  in eq. (3.11) and also  $\Delta M^{gq}(N, Q^2)$  which is the quark-to-gluon evolution function, are given in ref. [25].

It is obvious that the final form for  $g_1(N, Q^2)$  involves the total of 15 unknown parameters. If the parameters can be obtained then the computation of all moments of the PPDFs and the polarized structure function (PSF),  $g_1(N, Q^2)$ , are possible.

#### 4. The method of the QCD analysis of PSF

The evolution equations allow one to calculate the  $Q^2$ -dependence of the PPD's provided at a certain reference point  $Q_0^2$ . These distributions are usually parameterized on the basis of plausible theoretical assumptions concerning their behavior near the end points  $x = 0, 1$ .

In the phenomenological investigations of the polarized and unpolarized structure functions, for example  $xg_1^p$  or  $xF_3^p$  for a given value of  $Q^2$ , only a limited number of experimental points, covering a partial range of values of  $x$ , are available. Therefore, one cannot directly determine the moments. A method devised to deal with this situation is to take averages of the structure function weighted by suitable polynomials.

The evolution equation can be solved and QCD predictions for PSF obtained with the help of various methods. For example we can use the Bernstein polynomial to determine PPD's in the NLO approximation to obtain some unknown parameters to parameterize PPD's at  $Q_0^2$ . In this way, we can compare theoretical predictions with the experimental results for the Bernstein averages just in MELLIN- $N$  space. To obtain these experimental averages from the E143 and SMC data [51, 52], we need to fit  $xg_1(x, Q^2)$  for each bin in  $Q^2$  separately [25].

If we want to take into account very recent experimental data [47] for all range value of  $Q^2$  to determine PPDFs, it is convenience to apply Jacobi polynomials expansion and not the Bernstein one. The advantage of application for all data points, especially very recently HERMES experimental data [47], and not just a series of data points, is our motivation to use Jacobi polynomials and not Bernstein polynomial to study spin dependent of parton distribution function.

One of the simplest and fastest possibilities in the PSF reconstruction from the QCD predictions for its Mellin moments is Jacobi polynomials expansion. The Jacobi polynomials are especially suited for this purpose since they allow one to factor out an essential part of the  $x$ -dependence of the SF into the weight function [53]. Thus, given the Jacobi moments  $a_n(Q^2)$ , a structure function  $f(x, Q^2)$  may be reconstructed in a form of the series [54]–[58]

$$xf(x, Q^2) = x^\beta(1-x)^\alpha \sum_{n=0}^{N_{\max}} a_n(Q^2) \Theta_n^{\alpha, \beta}(x), \quad (4.1)$$



where  $N_{\max}$  is the number of polynomials and  $\Theta_n^{\alpha,\beta}(x)$  are the Jacobi polynomials of order  $n$ ,

$$\Theta_n^{\alpha,\beta}(x) = \sum_{j=0}^n c_j^{(n)}(\alpha, \beta) x^j, \quad (4.2)$$

where  $c_j^{(n)}(\alpha, \beta)$  are the coefficients that expressed through  $\Gamma$ -functions and satisfy the orthogonality relation with the weight  $x^\beta(1-x)^\alpha$  as following

$$\int_0^1 dx x^\beta(1-x)^\alpha \Theta_k^{\alpha,\beta}(x) \Theta_l^{\alpha,\beta}(x) = \delta_{k,l}, \quad (4.3)$$

For the moments, we note that the  $Q^2$  dependence is entirely contained in the Jacobi moments

$$\begin{aligned} a_n(Q^2) &= \int_0^1 dx x f(x, Q^2) \Theta_k^{\alpha,\beta}(x) \\ &= \sum_{j=0}^n c_j^{(n)}(\alpha, \beta) f(j+2, Q^2). \end{aligned} \quad (4.4)$$

obtained by inverting eq. 4.1, using eqs. (4.2), (4.3) and also definition of moments,  $f(j, Q^2) = \int_0^1 dx x^{j-2} x f(x, Q^2)$ .

Using eqs. (4.1), (4.4) now, one can relate the PSF with its Mellin moments

$$xg_1^{N_{\max}}(x, Q^2) = x^\beta(1-x)^\alpha \sum_{n=0}^{N_{\max}} \Theta_n^{\alpha,\beta}(x) \sum_{j=0}^n c_j^{(n)}(\alpha, \beta) g_1(j+2, Q^2), \quad (4.5)$$

where  $g_1(j+2, Q^2)$  are the moments determined by eqs. (3.2), (3.5).  $N_{\max}$ ,  $\alpha$  and  $\beta$  have to be chosen so as to achieve the fastest convergence of the series on the r.h.s. of eq. (4.5) and to reconstruct  $xg_1$  with the required accuracy. In our analysis we use  $N_{\max} = 9$ ,  $\alpha = 3.0$  and  $\beta = 0.5$ . The same method has been applied to calculate the nonsinglet structure function  $x F_3$  from their moments [59-63].

Obviously the  $Q^2$ -dependence of the polarized structure function is defined by the  $Q^2$ -dependence of the moments.

## 5. The procedure of the QCD fit of $g_1^p$ data

The remarkable growth of experimental data on inclusive polarized deep inelastic scattering of leptons off nucleons over the last years allows to perform refined QCD analyzes of polarized structure functions in order to reveal the spin-dependent partonic structure of the nucleon. For the QCD analysis presented in the present paper the following data sets are used: the HERMES proton data [64, 47], the SMC proton data [65], the E143 proton data [51], the EMC proton data [66, 67]. The number of the published data points above  $Q^2 = 1.0 \text{ GeV}^2$  for the different data sets are summarized in table 1 for data on  $g_1$  together with the  $x$ - and  $Q^2$ -ranges for different experiments.

In the fitting procedure we started with the 15 parameters selected, i.e. 4 parameters for each non-singlet polarized valon distribution, 6 parameters for singlet polarized

| Experiment | $x$ -range    | $Q^2$ -range<br>[GeV <sup>2</sup> ] | number of data points | ref. |
|------------|---------------|-------------------------------------|-----------------------|------|
| E143(p)    | 0.031 – 0.749 | 1.27 – 9.52                         | 28                    | [51] |
| E143(p)    | 0.031 – 0.749 | 2, 3, 5 (Fixed)                     | 84                    | [51] |
| HERMES(p)  | 0.028 – 0.660 | 1.01 – 7.36                         | 19                    | [64] |
| HERMES(p)  | 0.023 – 0.660 | 2.5 (Fixed)                         | 20                    | [64] |
| HERMES(p)  | 0.026 – 0.731 | 1.12-14.29                          | 62                    | [47] |
| SMC(p)     | 0.005 – 0.480 | 1.30 – 58.0                         | 12                    | [65] |
| SMC(p)     | 0.005 – 0.480 | 10 (Fixed)                          | 12                    | [65] |
| EMC(p)     | 0.015 – 0.466 | 3.50 – 29.5                         | 10                    | [66] |
| EMC(p)     | 0.015 – 0.466 | 3.50 – 29.5                         | 10                    | [67] |
| proton     |               |                                     | 257                   |      |

**Table 1:** Published data points above  $Q^2 = 1.0 \text{ GeV}^2$ .

valon distribution and  $\Lambda_{\text{QCD}}$  to be determined. For this set of parameters the sea-quark distribution was assumed to be described according to SU(3) flavor symmetry.

In the further procedure we fixed 2 parameters at their values obtained in the first minimization and chose the first moment of polarized Non-singlet valon distributions in the polarized case [25]. The lack of constraining power of the present data on the polarized parton densities has to be stressed, however. Since only more precise data can improve the situation, so we add the recent experimental data achieved from HERMES group [47].

The final minimization was carried out under the above conditions and determined the remaining 15 parameters. The values and errors of these parameters along with those parameters fixed in the parametrization, section 2, are summarized in LO and NLO in table 2. The results on  $\Lambda_{\text{QCD}}$  are discussed separately in section 6. The starting scale of the evolution was chosen as  $Q_0^2 = 1 \text{ GeV}^2$ .

Using the CERN subroutine MINUIT [68], we defined a global  $\chi^2$  for all the experimental data points and found an acceptable fit with minimum  $\chi^2/\text{d.o.f.} = 236.577/242 = 0.978$  in the LO case and  $\chi^2/\text{d.o.f.} = 225.920/242 = 0.933$  in the NLO case. In this table we compare the results reported in [25] which are based on Bernstein approach and the results of the present analysis. Also we obtain the uncertainties of the parameters in Jacobi Approach which are not calculated in Bernstein approach. We should notice that the Jacobi and Bernstein polynomials are merely used as a tool in the fitting procedure and the results are independent of it.

## 6. Results and conclusions of the QCD analysis

We have performed a QCD analysis of the inclusive polarized deep-inelastic charged lepton-nucleon scattering data to next-to-leading order and derived parameterizations of polarized valon distributions at a starting scale  $Q_0^2$  together with the QCD-scale  $\Lambda_{\text{QCD}}$  in the polarized valon model framework.

|  | Bernstein Approach [25] |                    | Jacobi Approach      |                      |
|--|-------------------------|--------------------|----------------------|----------------------|
|  | LO                      | NLO                | LO                   | NLO                  |
|  | value                   | value              | value                | value                |
| $\Lambda_{\text{QCD}}^{(4)}; \text{MeV}$ | 203                     | 235                | $201 \pm 110$        | $245 \pm 58$         |
| $N_U (= \xi_U A_U)$                      | 0.0020                  | 0.0038             | 0.0015(fixed)        | 0.0018(fixed)        |
| $\alpha_U$                               | -2.3789                 | -2.1501            | $-2.4489 \pm 0.024$  | $-2.3590 \pm 0.028$  |
| $\beta_U$                                | -1.7518                 | -0.8859            | $-1.9050 \pm 0.196$  | $-0.9683 \pm 0.206$  |
| $\gamma_U$                               | 11.0804                 | 10.6537            | $13.5420 \pm 0.378$  | $22.6095 \pm 0.418$  |
| $\eta_U$                                 | -1.4629                 | -0.1548            | $-1.8339 \pm 0.120$  | $-1.9778 \pm 0.150$  |
| $N_D (= \xi_D A_D)$                      | -0.005                  | -0.0046            | -0.0029(fixed)       | -0.0026(fixed)       |
| $\alpha_D$                               | -1.5465                 | -1.5859            | $-1.6059 \pm 0.029$  | $-1.6638 \pm 0.034$  |
| $\beta_D$                                | -1.8776                 | -1.5835            | $-2.2009 \pm 0.353$  | $-1.6214 \pm 0.453$  |
| $\gamma_D$                               | 8.5042                  | 9.6205             | $10.2371 \pm 0.829$  | $13.1966 \pm 0.942$  |
| $\eta_D$                                 | -0.8608                 | -0.8410            | $0.8751 \pm 0.091$   | $0.8483 \pm 0.142$   |
| $\mathcal{A}_0$                          | 0.0004                  | -0.0025            | $0.0003 \pm 10^{-5}$ | $0.0052 \pm 10^{-5}$ |
| $\mathcal{A}_1$                          | 0.2954                  | -3.1148            | $0.2611 \pm 0.191$   | $-3.0034 \pm 0.241$  |
| $\mathcal{A}_2$                          | -6.9134                 | 15.8114            | $-6.5429 \pm 0.174$  | $14.8696 \pm 0.214$  |
| $\mathcal{A}_3$                          | 30.9851                 | -21.1500           | $29.6999 \pm 0.475$  | $-18.8057 \pm 0.051$ |
| $\mathcal{A}_4$                          | -39.7383                | 10.5025            | $-37.9379 \pm 0.202$ | $8.4598 \pm 0.298$   |
| $\mathcal{A}_5$                          | 16.4605                 | -0.9162            | $15.5879 \pm 0.041$  | $-0.3410 \pm 0.050$  |
| $\chi^2/ndf$                             | $154.98/123=1.260$      | $115.62/123=0.940$ | $236.577/242=0.978$  | $225.920/242=0.933$  |

**Table 2:** Parameter values in LO and NLO of the parameter fit for Bernstein and Jacobi approaches.

The analysis was performed using the Jacobi polynomials-method to determine the parameters of the problem in a fit to the data.

A new aspect in comparison with previous analyzes is that we determine the parton densities and the QCD scale in leading and next-to-leading order by using Jacobi polynomial expansion method.

Detailed comparisons were performed to the results obtained in other recent parameterizations [24, 23, 20, 27, 26]. The previous results are widely compatible with the present parameterizations. These distributions can be used in the numerical calculations for polarized high-energy scattering processes at hadron- and  $ep$ -colliders.

Looking at the  $Q^2$  dependence of the structure function  $g_1(x, Q^2)$  in intervals of  $x$  gives insight to the scaling violations in the spin sector. As in the unpolarized case the presence of scaling violations are expected to manifest in a slope changing with  $x$ . The proton data on  $g_1(x, Q^2)$  have been plotted in such a way in figure 1 and confronted with the QCD NLO curves of the present analysis. Corresponding curves of the parameterizations [24, 23, 20, 27, 26] are also shown. Slight but non-significant differences between the different analyzes are observed in the intervals at low values of  $x$ . However, the data are well covered within the errors by all analyzes.

In figures 2–3 the fitted parton distribution functions, in leading and next-to-leading

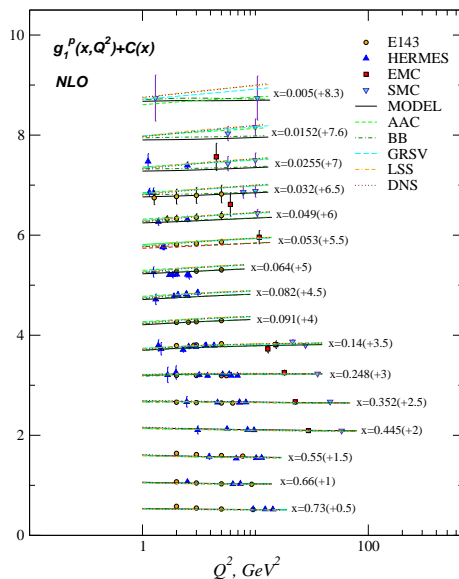


**Figure 1:** The polarized structure function  $g_1^p$  as function of  $Q^2$  in intervals of  $x$ . The error bars shown are the statistical and systematic uncertainties added in quadrature. The data are well described by our QCD NLO curves (solid lines) which based on the valon model and Jacobi polynomials expansion method. The values of  $C(x)$  are given in parentheses. Also shown are the QCD NLO curves obtained by AAC (dashed lines) [24], BB (dashed-dotted lines) [23], GRSV (long-dashed lines) [20], LSS (dashed-dashed-dotted lines) [27] and DNS (dotted lines) [26] for comparison.

order for all sets of parameterizations [24, 23, 20, 27] and their errors are presented at the starting scale  $Q_0^2$ .

The polarized structure function  $xg_1^p(x, Q^2)$  measured in the interval  $3.0 \text{ GeV}^2 < Q^2 < 5.0 \text{ GeV}^2$ , figure 4, using the world asymmetry data is well described by our QCD NLO curve. We also compare to corresponding representations of the parameterizations [27, 20, 23, 24], which are compatible within the present results.

In figures 5–8 the scaling violations of the individual polarized momentum densities are depicted in the range  $x \in [10^{-3}, 1]$ ,  $Q^2 \in [1, 10^4] \text{ GeV}$  choosing the NLO distributions. The up-valence distribution  $x\Delta u_v$ , figure 5, evolves towards smaller values of  $x$  and the peak around  $x \sim 0.25$  becomes more flat in the evolution from  $Q^2 = 1 \text{ GeV}^2$  to  $Q^2 = 10^4 \text{ GeV}^2$ . Statistically this distribution is constrained best among all others. The down-valence distribution  $x\Delta d_v$ , figure 6, remains negative in the same range, although it is less constraint by the present data than the up-valence density. Also here the evolution is towards smaller values of  $x$  and structures at larger  $x$  flatten out.

The momentum density of the polarized singlet quark  $x\Delta\Sigma$ , figure 7, is positive in the kinematic range shown for all  $Q^2$  and for  $x \geq 0.1$ , but changes sign for lower values of  $x$ . The maximum of the distribution at  $Q^2 = 1 \text{ GeV}^2$  around  $x \sim 0.3$  moves to  $x \sim 0.2$  at  $Q^2 = 10^4 \text{ GeV}$ . At the same time a minimum around  $x \sim 0.03$  moves to  $x \sim 0.002$ .

The momentum density of the polarized gluon  $x\Delta G$ , figure 8, is positive in the kine-

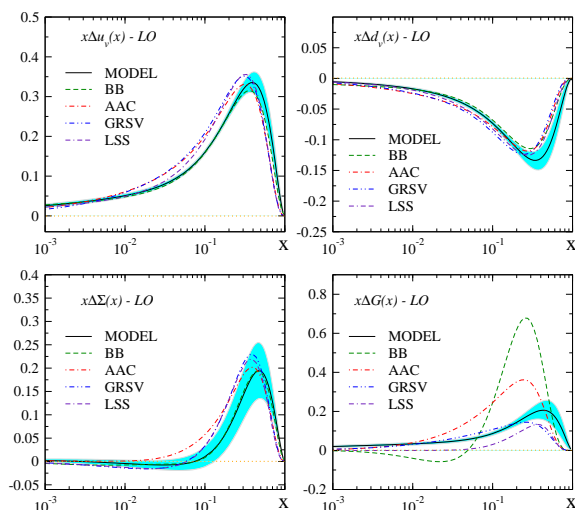


**Figure 2:** LO polarized parton distributions at the input scale  $Q_0^2=1.0\text{ GeV}^2$  compared to results obtained by BB model (dashed line) (ISET=1) [23], AAC (dashed-dotted line) (ISET=1) [24], GRSV (dashed-dotted dotted line) (ISET=3) [20] and LSS (dashed-dashed dotted line) (ISET=1)

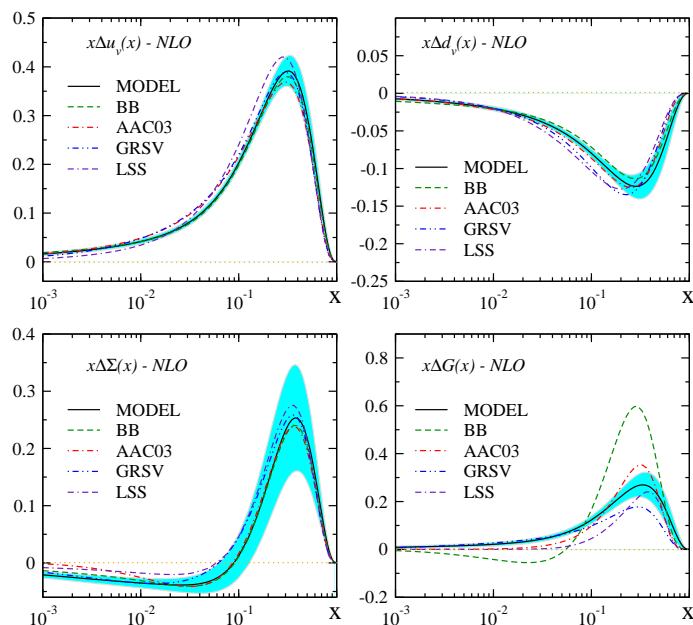


**Figure 3:** NLO polarized parton distributions at the input scale  $Q_0^2=1.0\text{ GeV}^2$  compared to results obtained by BB model (dashed line) (ISET=3) [23], AAC (dashed-dotted line) (ISET=3) [24], GRSV (dashed-dotted dotted line) (ISET=1) [20] and LSS (dashed-dashed dotted line) (ISET=1) [27]

matic range shown for all  $Q^2$ . Also in this case the evolution moves the shape towards lower values of  $x$  and flattens the distribution.

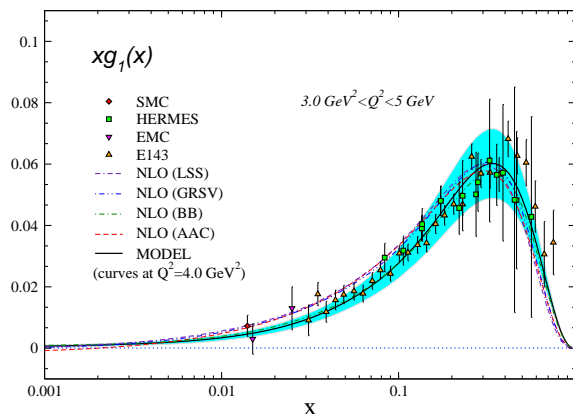


**Figure 4:** Polarized proton structure function  $xg_1^p$  measured in the interval  $3.0 \text{ GeV}^2 < Q^2 < 5.0 \text{ GeV}^2$  as a function of  $x$ . Also shown are the QCD NLO curves at the same value of  $Q^2$  obtained by LSS (dashed-dashed dotted line) (ISET=1) [27], GRSV (dashed-dotted dotted line) (ISET=1) [20], BB model (dashed-dotted line) (ISET=3) [23] and AAC (dashed line) (ISET=3) [24] for compar

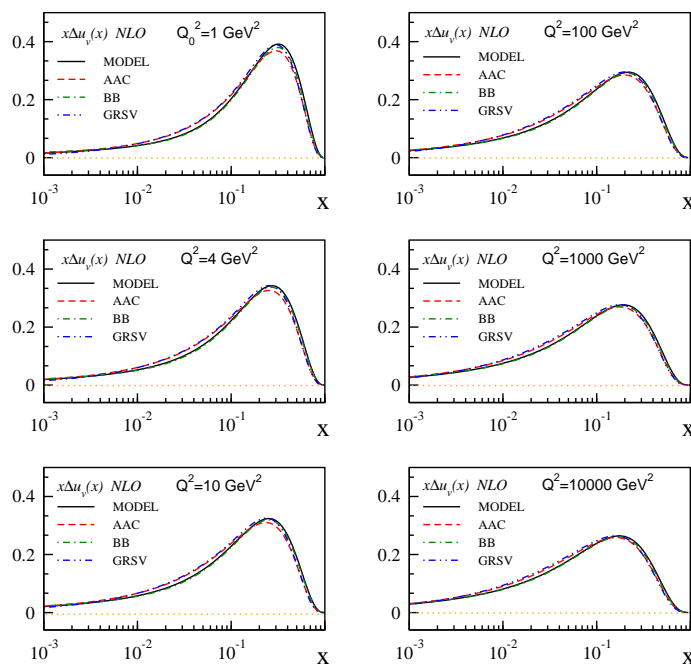


**Figure 5:** The Polarized parton distribution  $x\Delta u_v$ , evolved up to values of  $Q^2=10,000 \text{ GeV}^2$  as a function of  $x$  in the NLO approximation. The solid line is our model, dashed line is the AAC model (ISET=3) [24], dashed-dotted line is the BB model (ISET=3) [23] and dashed-dotted-dotted line is the GRSV model (ISET=1) [20].

By having polarized parton distributions, the first moments of the polarized parton distributions can be obtain. The first moments of the polarized parton densities in NLO

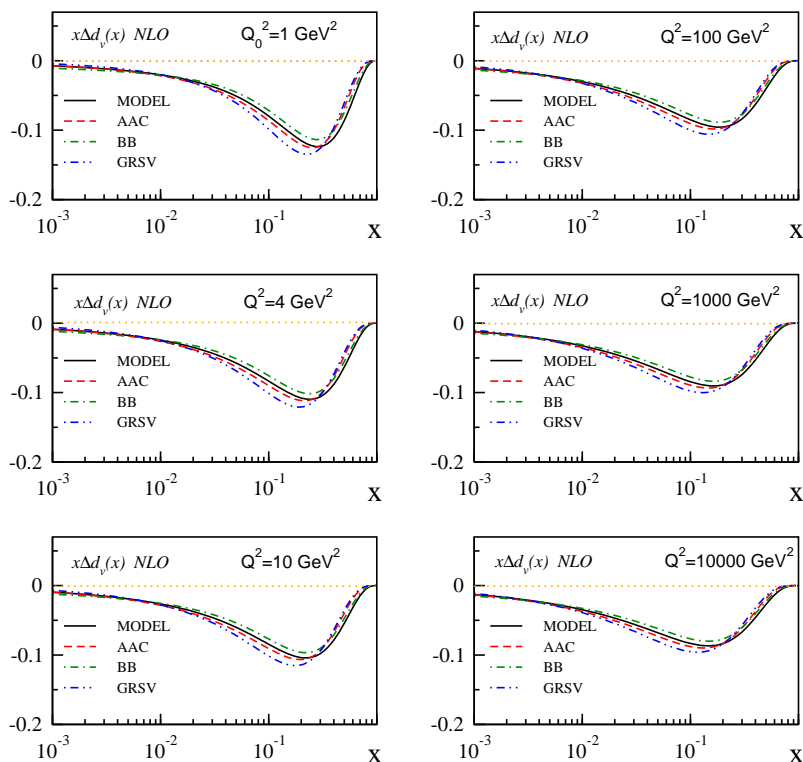


**Figure 6:** The Polarized parton distribution  $x\Delta d_v$ , evolved up to values of  $Q^2=10,000 \text{ GeV}^2$  as a function of  $x$  in the NLO approximation. The solid line is our model, dashed line is the AAC model (ISET=3) [24], dashed-dotted line is the BB model (ISET=3) [23] and dashed-dotted-dotted line is the GRSV model (ISET=1) [20].

| Distribution     | Model   | ref. [25] | BB [23] | GRSV [20] | AAC [24] |
|------------------|---------|-----------|---------|-----------|----------|
| $\Delta u_v$     | 0.9207  | 0.8769    | 0.926   | 0.9206    | 0.9278   |
| $\Delta d_v$     | -0.3391 | -0.3313   | -0.341  | -0.3409   | -0.3416  |
| $\Delta u$       | 0.8390  | 0.8145    | 0.851   | 0.8593    | 0.8399   |
| $\Delta d$       | -0.4207 | -0.3937   | -0.415  | -0.4043   | -0.4295  |
| $\Delta \bar{q}$ | -0.0817 | -0.0624   | -0.074  | -0.0625   | -0.0879  |
| $\Delta G$       | 0.9325  | 0.8322    | 1.026   | 0.6828    | 0.8076   |

**Table 3:** Comparison of the first moments of the polarized parton densities in NLO in the  $\overline{\text{MS}}$  scheme at  $Q^2 = 4 \text{ GeV}^2$  for different sets of recent parton parameterizations. The second column (Model) contains the first moments which is obtained from the valon model and the Jacobi polynomials expansion method.

in the  $\overline{\text{MS}}$  scheme at  $Q^2 = 4 \text{ GeV}^2$  for different sets of recent parton parameterizations are presented in table 3.

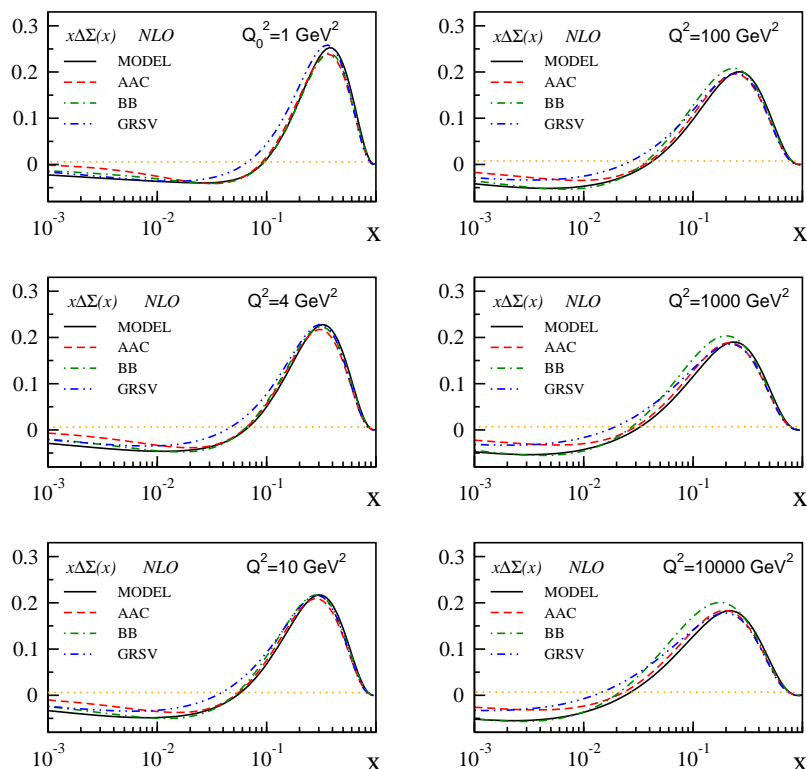


**Figure 7:** The Polarized parton distribution  $x\Delta\Sigma$ , evolved up to values of  $Q^2=10,000 \text{ GeV}^2$  as a function of  $x$  in the NLO approximation. The solid line is our model, dashed line is the AAC model (ISET=3) [24], dashed-dotted line is the BB model (ISET=3) [23] and dashed-dotted-dotted line is the GRSV model (ISET=1) [20].

| $Q^2(\text{GeV}^2)$ | $\Delta u_v$ | $\Delta d_v$ | $\Delta\Sigma$ | $\Delta\bar{q}$ | $\Delta g$ | $\Gamma_1^p$ |
|---------------------|--------------|--------------|----------------|-----------------|------------|--------------|
| 1                   | 0.9260       | -0.3410      | 0.0965         | -0.0814         | 0.5850     | 0.1161       |
| 3                   | 0.9215       | -0.3393      | 0.0923         | -0.0816         | 0.8651     | 0.1195       |
| 5                   | 0.9202       | -0.3389      | 0.0911         | -0.0817         | 0.9837     | 0.1205       |
| 10                  | 0.9189       | -0.3384      | 0.0898         | -0.0818         | 1.1383     | 0.1215       |

**Table 4:** The first moments of polarized parton distributions,  $\Delta u_v$ ,  $\Delta d_v$ ,  $\Delta\Sigma$ ,  $\Delta\bar{q}$ ,  $\Delta g$  and  $\Gamma_1^p$  in the NLO approximation for some value of  $Q^2$ .

We can also obtain the first moment of  $g_1^p$  (the Ellis-Jaffe sum rule) by

$$\Gamma_1^p(Q^2) \equiv \int_0^1 dx g_1^p(x, Q^2). \tag{6.1}$$

The results have also been given in table 4. The first moments of polarized parton distributions also shown for some value of  $Q^2$ .

In the framework of QCD the spin of the proton can be expressed in terms of the first moment of the total quark and gluon helicity distributions and their orbital angular



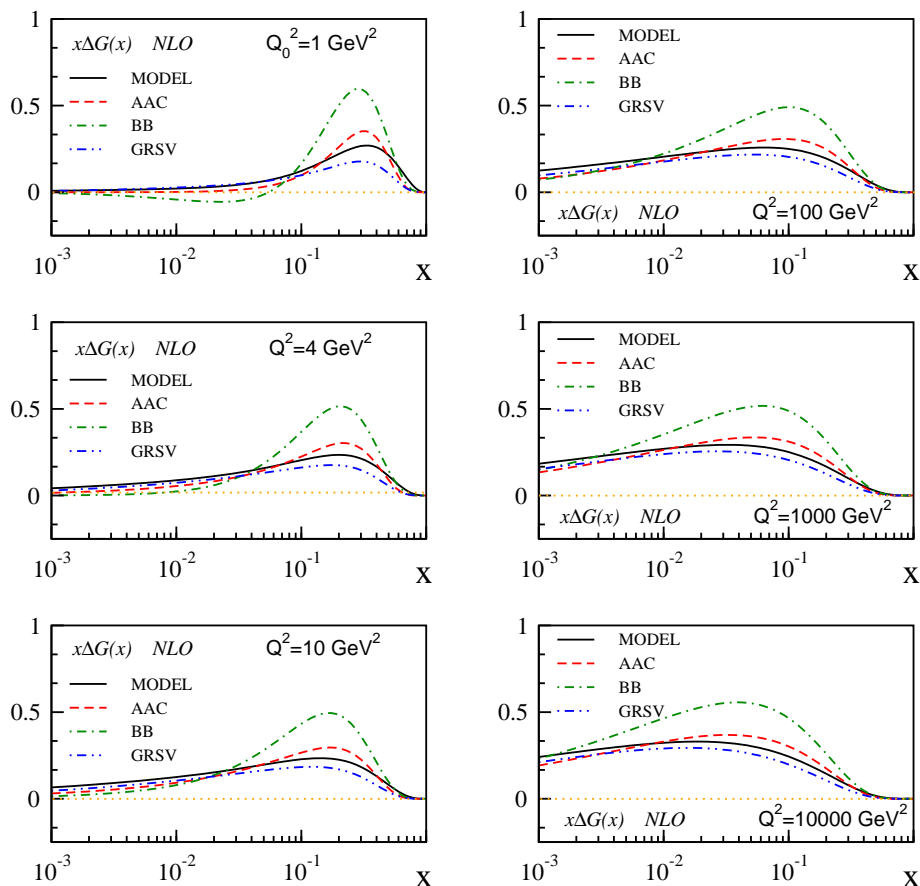


**Figure 8:** The Polarized parton distribution  $x\Delta G$ , evolved up to values of  $Q^2=10,000\text{ GeV}^2$  as a function of  $x$  in the NLO approximation. The solid line is our model, dashed line is the AAC model (ISET=3) [24], dashed-dotted line is the BB model (ISET=3) [23] and dashed-dotted-dotted line is the GRSV model (ISET=1) [20].

momentum, i.e.

$$\frac{1}{2} = \frac{1}{2}\Delta\Sigma^p + \Delta g^p + L_z^p, \tag{6.2}$$

where  $L_z^p$  is the total orbital angular momentum of all the quarks and gluons. The contribution of addition of  $\frac{1}{2}\Delta\Sigma$  and  $\Delta g$  for typical value of  $Q^2 = 4\text{ GeV}^2$  is around 0.978 in our analysis. We can also compare this value in NLO with other recent analysis. The reported value from BB model [23] is 1.096, AAC model [24] is 0.837 and also GRSV model [20] is 0.785.

In the QCD analysis we parameterized the strong coupling constant  $\alpha_s$  in terms of four massless flavors determining  $\Lambda_{\text{QCD}}$ . The LO and NLO results fitting the data, are

$$\begin{aligned} \Lambda_{\text{QCD}}^{(4)\overline{\text{MS}}} &= 201 \pm 110(\text{stat}) \text{ MeV, LO,} \\ \Lambda_{\text{QCD}}^{(4)\overline{\text{MS}}} &= 245 \pm 58(\text{stat}) \text{ MeV, NLO,} \end{aligned} \tag{6.3}$$

These results can be expressed in terms of  $\alpha_s(M_Z^2)$ :

$$\begin{aligned}\alpha_s(M_Z^2) &= 0.1281 \pm 0.0094(stat) \text{ MeV, LO,} \\ \alpha_s(M_Z^2) &= 0.1141 \pm 0.0036(stat) \text{ MeV, NLO.}\end{aligned}\tag{6.4}$$

These values can be compared with results from other QCD analyzes of polarized inclusive deep-inelastic scattering data

$$\begin{aligned}\text{E154 [8] : } & \alpha_s(M_Z^2) = 0.108 - 0.116, \\ \text{SMC [69] : } & \alpha_s(M_Z^2) = 0.121 \pm 0.002(stat), \\ \text{ABFR [10] : } & \alpha_s(M_Z^2) = 0.120 \begin{matrix} +0.004 \\ -0.005 \end{matrix} \text{ (exp)} \begin{matrix} +0.009 \\ -0.006 \end{matrix} \text{ (theor)}, \\ \text{BB [23] : } & \alpha_s(M_Z^2) = 0.113 \pm 0.004(stat), \quad (\text{ISET}=3),\end{aligned}\tag{6.5}$$

and with the value of the current world average

$$\alpha_s(M_Z^2) = 0.118 \pm 0.002 \quad [70] .\tag{6.6}$$

We hope our results of QCD analysis of structure functions in terms of Jacobi polynomials could be able to describe more complicated hadron structure functions. We also hope to be able to consider the symmetry breaking of polarized sea quarks by using the polarized structure function expansion in the Jacobi polynomials.

## Acknowledgments

We are especially grateful to G. Altarelli for fruitful suggestions and critical remarks. A.N.K. is grateful to A. L. Kataev for useful discussions and remarks during the visit to ICTP. I am grateful to the staff of this center for providing excellent conditions for work. A.N.K is grateful to CERN for their hospitality whilst he visited there and could amend this paper. We would like to thank M. Ghominejad and Z. Karamloo for reading the manuscript of this paper. We acknowledge the Institute for Studies in Theoretical Physics and Mathematics (IPM) for financially supporting this project. S.A.T. thanks Persian Gulf university for partial financial support of this project.

## References

- [1] M. Anselmino, A. Efremov and E. Leader, *The theory and phenomenology of polarized deep inelastic scattering*, *Phys. Rept.* **261** (1995) 1 [[hep-ph/9501369](#)].
- [2] B. Lampe and E. Reya, *Spin physics and polarized structure functions*, *Phys. Rept.* **332** (2000) 1 [[hep-ph/9810270](#)].
- [3] E.W. Hughes and R. Voss, *Spin structure functions*, *Ann. Rev. Nucl. Part. Sci.* **49** (1999) 303.
- [4] B.W. Filippone and X.-D. Ji, *The spin structure of the nucleon*, *Adv. Nucl. Phys.* **26** (2001) 1 [[hep-ph/0101224](#)].

- [5] M. Gluck, E. Reya, M. Stratmann and W. Vogelsang, *Next-to-leading order radiative parton model analysis of polarized deep inelastic lepton-nucleon scattering*, *Phys. Rev. D* **53** (1996) 4775 [[hep-ph/9508347](#)].
- [6] M. Gluck, E. Reya, M. Stratmann and W. Vogelsang, *Next-to-leading order radiative parton model analysis of polarized deep inelastic lepton-nucleon scattering*, *Phys. Rev. D* **53** (1996) 4775 [[hep-ph/9508347](#)];  
M. Gluck, E. Reya and W. Vogelsang, *Radiative parton model analysis of polarized deep inelastic lepton-nucleon scattering*, *Phys. Lett. B* **359** (1995) 201 [[hep-ph/9507354](#)].
- [7] T. Gehrmann and W.J. Stirling, *Polarized parton distributions in the nucleon*, *Phys. Rev. D* **53** (1996) 6100 [[hep-ph/9512406](#)].
- [8] E154 collaboration, K. Abe et al., *Next-to-leading order QCD analysis of polarized deep inelastic scattering data*, *Phys. Lett. B* **405** (1997) 180 [[hep-ph/9705344](#)].
- [9] G. Altarelli, R.D. Ball, S. Forte and G. Ridolfi, *Determination of the Bjorken sum and strong coupling from polarized structure functions*, *Nucl. Phys. B* **496** (1997) 337 [[hep-ph/9701289](#)].
- [10] G. Altarelli, R.D. Ball, S. Forte and G. Ridolfi, *Theoretical analysis of polarized structure functions*, *Acta Phys. Polon. B* **29** (1998) 1145 [[hep-ph/9803237](#)].
- [11] R.D. Ball, G. Ridolfi, G. Altarelli and S. Forte, *What can we learn from polarized structure function data?*, [hep-ph/9707276](#).
- [12] C. Bourrely, F. Buccella, O. Pisanti, P. Santorelli and J. Soffer, *Polarized quarks, gluons and sea in nucleon structure functions*, *Prog. Theor. Phys.* **99** (1998) 1017 [[hep-ph/9803229](#)].
- [13] D. de Florian, O.A. Sampayo and R. Sassot, *Next-to-leading order analysis of inclusive and semi-inclusive polarized data*, *Phys. Rev. D* **57** (1998) 5803 [[hep-ph/9711440](#)].
- [14] L.E. Gordon, M. Goshtasbpour and G.P. Ramsey, *x-dependent polarized parton distributions*, *Phys. Rev. D* **58** (1998) 094017 [[hep-ph/9803351](#)].
- [15] E. Leader, A.V. Sidorov and D.B. Stamenov, *A new study of the polarized parton densities in the nucleon*, *Phys. Lett. B* **462** (1999) 189 [[hep-ph/9905512](#)]; *Scheme dependence in polarized deep inelastic scattering*, *Phys. Lett. B* **445** (1998) 232 [[hep-ph/9808248](#)]; *Polarized parton densities in the nucleon*, *Phys. Rev. D* **58** (1998) 114028 [[hep-ph/9807251](#)]; *Nlo QCD analysis of polarized deep inelastic scattering*, *Int. J. Mod. Phys. A* **13** (1998) 5573 [[hep-ph/9708335](#)].
- [16] M. Stratmann, *GRSV parton densities revisited*, *Nucl. Phys.* **79** (Proc. Suppl.) (1999) 538 [[hep-ph/9907465](#)].
- [17] ASYMMETRY ANALYSIS collaboration, Y. Goto et al., *Polarized parton distribution functions in the nucleon*, *Phys. Rev. D* **62** (2000) 034017 [[hep-ph/0001046](#)].
- [18] D.K. Ghosh, S. Gupta and D. Indumathi, *A QCD analysis of polarised parton densities*, *Phys. Rev. D* **62** (2000) 094012 [[hep-ph/0001287](#)].
- [19] D. de Florian and R. Sassot, *Inclusive and semi-inclusive polarized DIS data revisited*, *Phys. Rev. D* **62** (2000) 094025 [[hep-ph/0007068](#)].
- [20] M. Gluck, E. Reya, M. Stratmann and W. Vogelsang, *Models for the polarized parton distributions of the nucleon*, *Phys. Rev. D* **63** (2001) 094005 [[hep-ph/0011215](#)].
- [21] R.S. Bhalariao, *Is the polarized anti-quark sea in the nucleon flavor symmetric?*, *Phys. Rev. D* **63** (2001) 025208 [[hep-ph/0003075](#)].

- [22] E. Leader, A.V. Sidorov and D.B. Stamenov, *A new evaluation of polarized parton densities in the nucleon*, *Eur. Phys. J. C* **23** (2002) 479 [[hep-ph/0111267](#)].
- [23] J. Bluemlein and H. Bottcher, *QCD analysis of polarized deep inelastic scattering data and parton distributions*, *Nucl. Phys. B* **636** (2002) 225 [[hep-ph/0203155](#)].
- [24] ASYMMETRY ANALYSIS collaboration, Y. Goto et al., *Polarized parton distribution functions in the nucleon*, *Phys. Rev. D* **62** (2000) 034017 [[hep-ph/0001046](#)];  
ASYMMETRY ANALYSIS collaboration, M. Hirai, S. Kumano and N. Saito, *Determination of polarized parton distribution functions and their uncertainties*, *Phys. Rev. D* **69** (2004) 054021 [[hep-ph/0312112](#)].
- [25] A.N. Khorramian, A. Mirjalili and S.A. Tehrani, *Next-to-leading order approximation of polarized valon and parton distributions*, *JHEP* **10** (2004) 062 [[hep-ph/0411390](#)].
- [26] D. de Florian, G.A. Navarro and R. Sassot, *Sea quark and gluon polarization in the nucleon at NLO accuracy*, *Phys. Rev. D* **71** (2005) 094018 [[hep-ph/0504155](#)].
- [27] E. Leader, A.V. Sidorov and D.B. Stamenov, *Longitudinal polarized parton densities updated*, *Phys. Rev. D* **73** (2006) 034023 [[hep-ph/0512114](#)].
- [28] A. Mirjalili, S. Atashbar Tehrani and A.N. Khorramian, *The role of polarized valons in the flavor symmetry breaking of nucleon sea*, *Int. J. Mod. Phys. A* **21** (2006) 4599 [[hep-ph/0608224](#)].
- [29] C.R.V. Bourrely, J. Soffer and F. Buccella, *The statistical parton distributions: status and prospects*, *Eur. Phys. J. C* **41** (2005) 327 [[hep-ph/0502180](#)]; *The extension to the transverse momentum of the statistical parton distributions*, *Mod. Phys. Lett. A* **21** (2006) 143 [[hep-ph/0507328](#)]; *Strangeness asymmetry of the nucleon in the statistical parton model*, *Phys. Lett. B* **648** (2007) 39 [[hep-ph/0702221](#)].
- [30] R.C. Hwa, *Leading and nonleading  $D^\pm$  production in the Valon model*, *Phys. Rev. D* **51** (1995) 85.
- [31] R.C. Hwa and M. Sajjad Zahir, *Proton fragmentation in deep inelastic scattering: a treatment in the valon recombination model*, *Z. Physik C* **20** (1983) 27.
- [32] R.C. Hwa, *Valon model for hadrons and their interactions*, presented at NATO Advanced Study Inst. on *Progress in Nuclear Dynamics*, Pearson Coll., B.C., Canada, Aug 23 - Sep 3 (1982).
- [33] R.C. Hwa, *Recent developments in the Valon model*, invited paper given at 13<sup>th</sup> *Int. Symp. on Multiparticle Dynamics*, Volendam, Netherlands, Jun 6-11 (1982).
- [34] BRUSSELS-CERN-GENOA-MONS-NIJMEGEN-SERPUKHOV collaboration, L. Gatignon, R.T. Van De Walle and R.C. Hwa, *Determination of kaon and Valon structures from soft hadronic processes*, talk.
- [35] R.C. Hwa, *Charm production in the Valon model*, *Phys. Rev. D* **27** (1983) 653.
- [36] R.C. Hwa, *Central production and small angle elastic scattering in the valon model*, invited paper given at 12<sup>th</sup> *Int. Symp. on Multiparticle Dynamics*, Notre Dame, Ind., Jul 21-26 (1981).
- [37] R.C. Hwa and M.S. Zahir, *Parton and valon distributions in the nucleon*, *Phys. Rev. D* **23** (1981) 2539.

- [38] R.C. Hwa, *Evidence for valence quark clusters in nucleon structure functions*, *Phys. Rev. D* **22** (1980) 759.
- [39] R.C. Hwa, *Clustering and hadronization of quarks: a treatment of the low  $P(T)$  problem*, *Phys. Rev. D* **22** (1980) 1593.
- [40] R.C. Hwa and C.B. Yang, *Parton distributions in the valon model*, *Phys. Rev. D* **66** (2002) 025204 [[hep-ph/0202140](#)]; *Inclusive distributions for hadronic collisions in the valon recombination model*, *Phys. Rev. D* **66** (2002) 025205 [[hep-ph/0204289](#)].
- [41] F. Arash and A.N. Khorramian, *Next-to-leading order constituent quark structure and hadronic structure functions*, *Phys. Rev. D* **67** (2003) 045201 [[hep-ph/0303031](#)].
- [42] F. Arash, *Pion structure function  $F_2(\pi)$  in the valon model*, *Phys. Lett. B* **557** (2003) 38 [[hep-ph/0301260](#)].
- [43] F. Arash, *Meson structure functions in the next-to-leading order valon model*, *Phys. Rev. D* **69** (2004) 054024 [[hep-ph/0307221](#)].
- [44] HERMES collaboration, A. Airapetian et al., *Quark helicity distributions in the nucleon for up, down and strange quarks from semi-inclusive deep-inelastic scattering*, *Phys. Rev. D* **71** (2005) 012003 [[hep-ex/0407032](#)].
- [45] COMPASS collaboration, G. Baum et al., *COMPASS: a proposal for a common muon and proton apparatus for structure and spectroscopy*, CERN-SPSLC-96-14 (1996).
- [46] SPIN MUON collaboration, B. Adeva et al., *Polarised quark distributions in the nucleon from semi-inclusive spin asymmetries*, *Phys. Lett. B* **420** (1998) 180 [[hep-ex/9711008](#)].
- [47] HERMES collaboration, A. Airapetian et al., *Precise determination of the spin structure function  $g(1)$  of the proton, deuteron and neutron*, [hep-ex/0609039](#).
- [48] G. Altarelli, N. Cabibbo, L. Maiani and R. Petronzio, *The nucleon as a bound state of three quarks and deep inelastic phenomena*, *Nucl. Phys. B* **69** (1974) 531.
- [49] PARTICLE DATA GROUP collaboration, C. Caso et al., *Review of particle physics*, *Eur. Phys. J. C* **3** (1998) 1.
- [50] G. Altarelli and G. Parisi, *Asymptotic freedom in parton language*, *Nucl. Phys. B* **126** (1977) 298.
- [51] E143 collaboration, K. Abe et al., *Measurements of the proton and deuteron spin structure functions  $g_1$  and  $g_2$* , *Phys. Rev. D* **58** (1998) 112003 [[hep-ph/9802357](#)];  
HERMES collaboration, A. Airapetian et al., *Measurement of the proton spin structure function  $g_1(p)$  with a pure hydrogen target*, *Phys. Lett. B* **442** (1998) 484 [[hep-ex/9807015](#)].
- [52] SPIN MUON (SMC) collaboration, D. Adams et al., *Spin structure of the proton from polarized inclusive deep-inelastic muon proton scattering*, *Phys. Rev. D* **56** (1997) 5330 [[hep-ex/9702005](#)].
- [53] G. Parisi and N. Surlas, *A simple parametrization of the  $Q^2$  dependence of the quark distributions in QCD*, *Nucl. Phys. B* **151** (1979) 421;  
I.S. Barker, C.S. Langensiepen and G. Shaw, *General parametrization of scale breaking*, *Nucl. Phys. B* **186** (1981) 61.

- [54] I.S. Barker, B.R. Martin and G. Shaw, *QCD analysis of nonsinglet neutrino structure functions*, *Z. Physik C* **19** (1983) 147;  
 I.S. Barker and B.R. Martin, *QCD analysis of nonsinglet electromagnetic structure functions*, *Z. Physik C* **24** (1984) 255;  
 S.P. Kurlovich, A.V. Sidorov and N.B. Skachkov, JINR Report E2-89-655, Dubna (1989).
- [55] V.G. Krivokhizhin et al., *QCD analysis of singlet structure functions using Jacobi polynomials: the description of the method*, *Z. Physik C* **36** (1987) 51.
- [56] V.G. Krivokhizhin et al., *Next-to-leading order QCD analysis of structure functions with the help of Jacobi polynomials*, *Z. Physik C* **48** (1990) 347.
- [57] J. Chyla and J. Rames, *On methods of analyzing scaling violation in deep inelastic scattering*, *Z. Physik C* **31** (1986) 151.
- [58] I.S. Barker, C.S. Langensiepen and G. Shaw, *General parametrization of scale breaking*, *Nucl. Phys. B* **186** (1981) 61.
- [59] A.L. Kataev, A.V. Kotikov, G. Parente and A.V. Sidorov, *Next-to-next-to-leading order QCD analysis of the revised CCFR data for  $xF_3$  structure function*, *Phys. Lett. B* **417** (1998) 374 [[hep-ph/9706534](#)].
- [60] A.L. Kataev, G. Parente and A.V. Sidorov, *The QCD analysis of the ccf data for  $xF_3$ : higher twists and  $\alpha_s(M_z)$  extractions at the nnlo and beyond*, [hep-ph/9809500](#).
- [61] S.I. Alekhin and A.L. Kataev, *The NLO dglap extraction of  $\alpha_s$  and higher twist terms from ccf  $xF_3$  and  $F_2$  structure functions data for  $\nu N$  DIS*, *Phys. Lett. B* **452** (1999) 402 [[hep-ph/9812348](#)].
- [62] A.L. Kataev, G. Parente and A.V. Sidorov, *Higher twists and  $\alpha_s(M_z)$  extractions from the NNLO QCD analysis of the CCFR data for the  $xF_3$  structure function*, *Nucl. Phys. B* **573** (2000) 405 [[hep-ph/9905310](#)].
- [63] A.L. Kataev, G. Parente and A.V. Sidorov, *Fixation of theoretical ambiguities in the improved fits to  $x f_3$  CCFR data at the next-to-next-to-leading order and beyond*, *Phys. Part. Nucl.* **34** (2003) 20 [[hep-ph/0106221](#)];  *$N^3LO$  fits to  $xF_3$  data:  $\alpha_s$  vs  $1/Q^2$  contributions*, *Nucl. Phys.* **116** (*Proc. Suppl.*) (2003) 105 [[hep-ph/0211151](#)];  
 A.L. Kataev, *The consequences of the relations between non-singlet contributions to  $g_1(N)$  and  $F_1(N)$  structure functions within infrared renormalon model*, [hep-ph/0306246](#); *Infrared renormalons and the relations between the Gross-Llewellyn smith and the Bjorken polarized and unpolarized sum rules*, *JETP Lett.* **81** (2005) 608 [*Zh. Eksp. Teor. Fiz.* **81** (2005) 744] [[hep-ph/0505108](#)].
- [64] HERMES collaboration, A. Airapetian et al., *Measurement of the proton spin structure function  $g_1(p)$  with a pure hydrogen target*, *Phys. Lett. B* **442** (1998) 484 [[hep-ex/9807015](#)].
- [65] SPIN MUON collaboration, B. Adeva et al., *Spin asymmetries  $a(1)$  and structure functions  $g_1$  of the proton and the deuteron from polarized high energy muon scattering*, *Phys. Rev. D* **58** (1998) 112001.
- [66] EUROPEAN MUON collaboration, J. Ashman et al., *A measurement of the spin asymmetry and determination of the structure function  $g(1)$  in deep inelastic muon proton scattering*, *Phys. Lett. B* **206** (1988) 364.

- [67] EUROPEAN MUON collaboration, J. Ashman et al., *An investigation of the spin structure of the proton in deep inelastic scattering of polarized muons on polarized protons*, *Nucl. Phys. B* **328** (1989) 1.
- [68] F. James and M. Roos, *Minuit: a system for function minimization and analysis of the parameter errors and correlations*, *Comput. Phys. Commun.* **10** (1975) 343.
- [69] SPIN MUON collaboration, B. Adeva et al., *A next-to-leading order QCD analysis of the spin structure function  $g_1$* , *Phys. Rev. D* **58** (1998) 112002.
- [70] PARTICLE DATA GROUP collaboration, D.E. Groom et al., *Review of particle physics*, *Eur. Phys. J. C* **15** (2000) 91.